Equilibrium and Dynamic Properties of Surface Gels Formed by Rigid-Rod Polypeptide Poly(γ-*n*-hexyl-α,L-glutamate)

Vladimir Kitaev and Eugenia Kumacheva*

Department of Chemistry, University of Toronto, 80 St. George Street, Toronto, Ontario, Canada M5S 3H6

Received September 13, 2002

ABSTRACT: Normal and shear forces acting in surface gels of rigid-rod polypeptide poly(γ-*n*-hexyl-α,L-glutamate) (PHLG) were studied using surface force balance with shear capability. The polymer was adsorbed to hydrophilic and hydrophobic surfaces providing strong and weak polymer−surface interactions, respectively. It was found that in both cases PHLG formed surface gels whose properties were dominated by polymer−surface rather than polymer−polymer interactions. On bare mica, PHLG formed a thick compact surface network whose properties were characterized by effective viscosity. In contrast, the surface gel formed on the hydrophobized surface had a weak structure and shear in this gel was dominated by surface slip. When long-time shear or high-velocity shear was applied to the adsorbed PHLG layers, the polymer underwent shear thinning, consistent with the nature of physical gel.

Introduction

Polymers with inherent rigidity associating through noncovalent cross-links represent a large group of biopolymers such as proteins, e.g., collagen and actin,[1] polysacharides,[2] and polypeptides.[3,4] Association of these polymers in solutions occurs through end-to-end or side-to-side aggregation of individual macromolecules. Following increase in polymer concentration, fibrils and bundles of fibrils are formed, which in moderately concentrated solutions form a three-dimensional network.

Associative rigid-rod macromolecules often have an amphiphilic nature and/or contain charges or dipoles in polymer backbone or in side chains; as a result, they adsorb as multilayers on various substrates. The equilibrium and dynamic interactions between these fluid multilayer assemblies govern important surface phenomena, such as stabilization, adhesion and friction of polymer-bearing surfaces, surface-induced gelation and fibrogenesis, and liquid flow past polymer-covered surfaces. Since polymer properties are determined by various compositional and structural factors that cannot be easily altered in a systematic way, the study of the surface-driven assembly of rigid biopolymers are not straightforward. Therefore, synthetic homopolymers of L-amino acids are often used as the relatively simple model systems. The investigation of adsorption of polyglutamates on various substrates, the surface alignment of α-helices, and the microstructure of thin polyglutamate films proved to be useful in understanding the principles of surface self-assembly and interfacial denaturation of proteins.

Among other synthetic polypeptides esters, the surface properties of poly(*n*-alkyl-L-glutamates) and poly(*n*-benzyl-L-glutamates) have been thoroughly investigated using dielectric spectroscopy,[5] quartz crystal resonator technique,[6] atomic force microscopy,[7] Brewster angle microscopy, and X-ray scattering.[8] The surface forces balance (SFB) technique[9] is a useful tool used in direct studies of intermolecular interactions between polymers adsorbed and/or confined between the two solid surfaces. Normal quasi-equilibrium forces acting between the two surfaces bearing polymers with inherent rigidity have been reported by several groups.[10−16] Most of these studies focused on adsorbed protein layers. Only Kurichara et al.[15] and Knoll et al.[16] studied intermolecular interactions between the surfaces bearing polyglutamic acid and its esters. The first group studied normal forces between the monolayers of poly(L-glutamic acid) adsorbed in brushlike configuration, while the second group examined adhesion and friction between the dry Langmuir−Blodgett films of laterally aligned poly(methyl-L-glutamate)-*co*-(*n*-octadecyl-L-glutamate) copolymer. In these studies, the role of the substrate in surface-induced polypeptide association was not examined, and the equilibrium and dynamic properties of *fluid supramolecular assemblies* of macromolecules were not addressed.

In the present study, we used the surface forces apparatus with shear capability to study the role of polymer−surface interactions on adsorption kinetics, equilibrium thickness, stability, and shear properties of adsorbed layers of a hairy-rod polymer poly(*n*-hexyl-L-glutamate). Two types of substrates were used: nonmodified mica and mica hydrophobized with octadecyltrichlorosilane. In earlier studies[7a,b] it was shown that poly(L-glutamates) strongly adsorb to charged hydrophilic mica while polymer adsorption to hydrophobized mica is weak, and the adsorbed layer can be easily removed from the surface by rinsing the substrate with a suitable solvent.

Experimental Section

Materials. Poly(γ-*n*-hexyl-α,L-glutamate) (PHLG) with M_v = 48 700 and M_w = 60 500, spectrograde toluene, chloroform, cyclohexane, and 95% octadecyltrichlorosilane (OTS) were supplied by Sigma-Aldrich Canada and used as received. Brownish muscovite grade 1 mica was purchased from S&J Trading. The water was passed through a Milli-Q water purification system and then distilled.

Sample Preparation. Mica was hydrophobized using a modified procedure of Granick et al.[17] A small amount of water of ca. 0.1 vol % was added to 5.7 ± 0.7 mM solution of OTS in cyclohexane cooled to 11 ± 0.5 °C. Immediately after addition of the water, the OTS solution was sonicated for 3 min. The mica sheets were glued to the silica glass lenses and immersed for ca. 12 min into the OTS solution. After silanization, the

10.1021/ma025675w CCC: $25.00
Published on Web 05/28/2003

surfaces were washed in chloroform and dried in the laminar flow cabinet. A contact angle of water on the hydrophobized mica plates was 93 ± 2°. The surface roughness of the OTS-modified mica surface was examined using atomic force microscopy (AFM, FM Pico SPM, Molecular Imaging, Phoenix, AZ). The mean roughness of the dry OTS layer measured in the contact mode (scan rate varying from 1 to 4 Hz; spring constant 0.06 or 0.12 N/m) was below ca. 0.5 nm with occasional minor defects not exceeding 1.5 nm.

Surface Force Measurements. The surface force balance technique with shear capability is described elsewhere.[9b,c] Briefly, two back-silvered mica sheets are glued onto two cylindrical silica glass lenses. The lenses are mounted opposite each other onto a flexible leaf spring (bottom surface) and a sectored piezoelectric tube PZT (top surface). The distance between the back-silvered mica surfaces, D, and the thickness of adsorbed layers are measured using white-light multiple-beam interferometry. The normal force, $F(D)$, between the polymer-covered surfaces is measured by monitoring the deflection, ΔD, of a flexible horizontal leaf spring supporting the lower lens as $F(D) = k_{\perp}\Delta D$, where $k_{\perp}$ is the spring constant. The results of these experiments are presented as a force−distance profile $F(D)/R$, where R is the mean radius of curvature of the surfaces. In our work, to minimize viscous drag, every experimental point was measured after, at least, 30−45 s equilibration. The lateral motion of the top surface, $\Delta x_0(t)$, was induced by applying potential to the opposite sectors of the PZT. The PZT was coupled with two vertical leaf springs; thus, the shear force, $F_{||}$, generated in the polymer layer was transmitted to the springs and measured as $F_{||}(D,t) = k_{||}\Delta x(t)$, where $\Delta x(t)$ is the time-dependent spring bending and $k_{||}$ is the vertical spring constant.[9b,c] The shear traces were recorded for various periods of time varying from 2 to 200 s using a Tektronix TDS 430A two-channel digital oscilloscope. All oscillatory shear measurements were performed in the range of frequencies not exceeding 5.0 Hz, that is, well below 17.3 Hz, the resonance frequency of the vertical springs.

Results

Normal Forces. Adsorption of PHLG on nonmodified mica (strong polymer−surface interaction) was studied by measuring quasi-equilibrium normal forces acting between the surfaces exposed to the PHLG solution for various time periods. To ensure that no contamination was present on the mica surface, prior to introducing the polymer solution into the experimental chamber, the force−distance profiles were measured between the mica plates immersed in a pure toluene. For $D > 60$ Å no forces acting between the surfaces were detected, while from $D \approx 60$ Å the surfaces moved into adhesive contact. Upon separation, the surfaces jumped apart due to a mechanical instability expected when $\partial F(D)/\partial D > k_{\perp}$. These results were consistent with previous findings.[18]

Following measurements in toluene, the solvent in the chamber was replaced with the polymer solution. The force−distance profiles measured in the solution are presented in Figure 1. Figure 1a shows the variation of normal force F/R vs D following exposure of bare mica to 0.5×10^{-4} g/mL polymer solution. For short adsorption time the forces between the surfaces were governed by repulsion commencing at $D \approx 200$ Å.[19] However, after 24 h incubation a weak attraction force appeared between the surfaces: from $D \approx 1300$ Å the surfaces slowly moved toward each other to $D \approx 500$ Å. The magnitude of attraction force was ca. 570 μN/m, measured on surface approach or separation, as is shown in the inset to Figure 1a. After additional 24 h equilibration no notable change in the force profiles was observed.

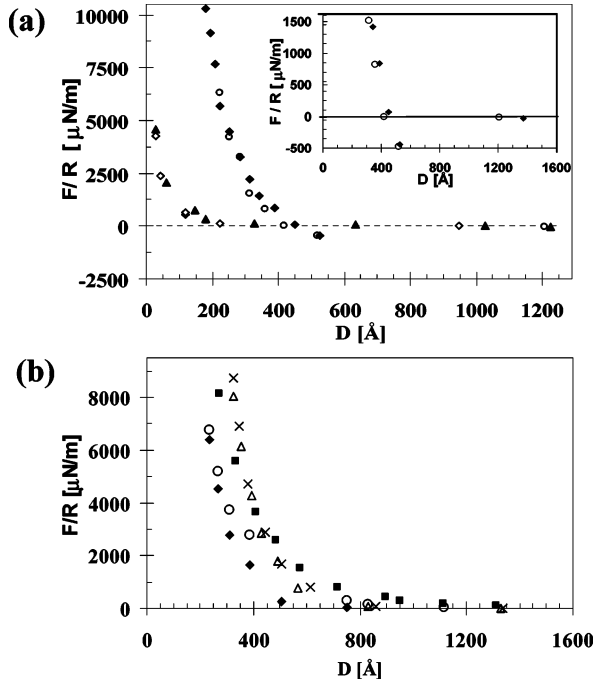

Figure 1. Normalized force−distance profiles measured on approach of mica surfaces incubated in PHLG solutions: **(**a**)** $c_{PHLG} = 0.5 \times 10^{-4}$ g/mL. Adsorption time: 1 h (◇), 3 h (▲), 24 h (○), 48 h (◆). Inset shows attraction forces measured on decompression of the polymer-covered surfaces following 24 h (○) and 48 h polymer adsorption. **(**b**)** $c_{PHLG} = 1.0 \times 10^{-4}$ g/mL; adsorption time: 1 h (◆), 2.5 h (○), 5 h (△), 8 h (×); $c_{PHLG} = 7.5 \times 10^{-5}$ g/mL, adsorption time 24 h (■).

Polymer adsorption was substantially faster for $c_{PHLG} \geq 1.0 \times 10^{-4}$ g/mL, as shown in Figure 1b. In this concentration regime, no attraction between the surfaces was noticed. After 1 h, a monotonic repulsion commenced at $D \approx 800$ Å. For the longer incubation times, the onset of repulsion force gradually shifted toward larger surface separation D, and the equilibrium layer thickness of 1370 ± 20 Å was achieved after 4 h incubation.[19] A further increase in c_{PHLG} to 7.5×10^{-4} g/mL did not change the thickness of the adsorbed layer and the magnitude of F/R. In all concentration regimes, the normal force profiles measured on approach and separation of the PHLG-covered mica showed no appreciable hysteresis.

The stability of the equilibrium PHLG adsorbed layers with respect to dilution was tested in a series of consecutive dilution experiments. Following the formation of the equilibrium adsorbed layer at $c_{PHLG} = 1.0 \times 10^{-4}$ g/mL, the polymer solution was consecutively diluted four times: in every step c_{PHLG} was reduced by a factor of 2. After each dilution step, the force profiles were measured after equilibration for at least 10 h. Figure 2 shows the variation in the normal force profiles following progressive dilution. For $c_{PHLG} > 0.25 \times 10^{-4}$ g/mL the surfaces featured repulsion upon compression and decompression, while for $c_{PHLG} = 0.25 \times 10^{-4}$ g/mL attraction appeared between the polymer-covered surfaces, and for $c_{PHLG} = 0.06 \times 10^{-4}$ g/mL the magnitude of attraction force reached ca. 270 μN/m. Attraction was somewhat weaker than that measured in adsorption experiments for $c_{PHLG} = 0.5 \times 10^{-4}$ g/mL (Figure 1a). In addition, following dilution to $c_{PHLG} = 0.06 \times 10^{-4}$ g/mL, the surface separation corresponding to $F/R \approx 8000$ μN/m was ca. 250 Å vs 220 Å measured for the equilibrium layer adsorbed from 0.5×10^{-4} g/mL

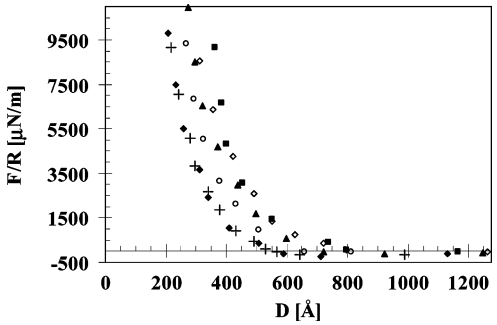

Figure 2. Normalized force−distance profiles measured on compression of PHLG layers following consecutive dilution of the bulk polymer solution: $c_{PHLG} = 1.0 \times 10^{-4}$ g/mL (■), $c_{PHLG} = 0.5 \times 10^{-4}$ g/mL (◇), $c_{PHLG} = 0.25 \times 10^{-4}$ g/mL (▲), $c_{PHLG} = 0.13 \times 10^{-4}$ g/mL (○), $c_{PHLG} = 0.06 \times 10^{-4}$ g/mL 17 h (+) and 40 h (◆) after dilution.

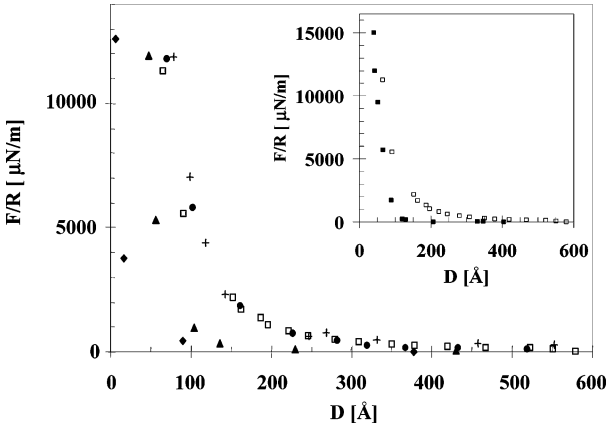

Figure 3. Normal force profiles measured on approach of OTS-modified surfaces following incubation in 0.5×10^{-4} g/mL PHLG solution for 1 h (◆), 4 h (▲), 24 h (●), 48 h (+) and in 7.0×10^{-4} g/mL PHLG solution for 48 h (□). Inset: compression (□) and decompression (■) force−distance profiles measured for the equilibrium PHLG layer adsorbed from 0.5×10^{-4} g/mL PHLG solution.

solution. Thus, although in dilution experiments c_{PHLG} was almost an order of magnitude lower than in experiments with ascending c_{pol}, a substantially thicker polymer layer remained on the surface. Even after 6 day desorption, the PHLG layer did not reach the thickness close to that measured in "direct" adsorption experiments.

Prior to experiments carried out on polymer layers adsorbed to hydrophobized mica (weak polymer−surface interactions), it was ensured that the OTS layer used for mica hydrophobization does not significantly change following its exposure to toluene. It was found that after 36 h incubation in toluene the thickness of the OTS layer increased from ca. 20 to 50 Å; that is, OTS underwent minor swelling.[19] From $D = 50$ Å the OTS layers could be compressed to ca. 20 Å by applying a strong compression force of 23 000 ± 3000 μN/m. The separation between the surfaces $D = 50$ Å was used as a reference point ($D = 0$) in the study of PHLG adsorbed to hydrophobized mica.

The force profiles measured between the hydrophobized surfaces immersed in 0.5×10^{-4} g/mL PHLG solutions for various periods of time are shown in Figure 3. No attraction between the surfaces was observed in these experiments. After 1 h adsorption, weak repulsion between the surfaces commenced at $D = 100$ Å; after 4 and 24 h incubation the onset of repulsion shifted to

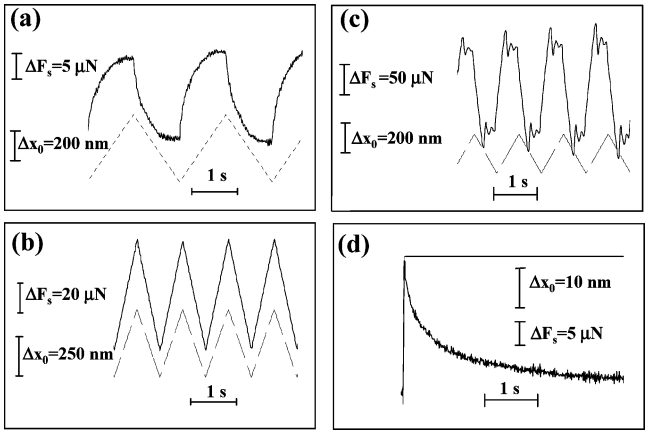

Figure 4. Shear forces between mica surfaces bearing adsorbed PHLG layers. In (a−c) the bottom traces show lateral displacement, Δx_0, applied to the layer as a function of time. The surfaces move with a constant velocity until the direction of shear is reversed. The top traces in (a−c) represent different types of shear response of the polymer layer upon increase in either shear displacement Δx_0 or decrease in confinement D: (a) the shear force in the layer increases until it reaches a plateau region at F_s; (b) the surfaces coupled through the polymer layer remain in rigid contact and the shear force in the polymer layer monotonically increases with an applied displacement; (c) the shear force increases until it reaches a critical value at which the polymer layer yields. From this point, the layer exhibits stick−slip motion. The shear force increases and decreases periodically, indicating solidification and liquification of the PHLG layer. The characteristic frequency of stick−slip is distinct from that of the vertical spring (17.3 Hz). (d) Relaxation experiment: Large lateral displacement, Δx_0, was rapidly applied to the layer (top trace) and the variation in shear force (bottom trace) was monitored in time.

ca. 230 and 550 Å, respectively. The latter layers could be compressed to $D \approx 80$ Å by applying forces of ca. 14 000 μN/m. In contrast to the PHLG layers adsorbed to bare mica, significant hysteresis was measured on approach and separation of the polymer-covered surfaces, as shown in the inset to Figure 3. After compression, the onset of repulsion forces moved from 550 to 200 Å, perhaps due to forced polymer adsorption caused by compression or partial expulsion of the polymer from the gap between the surfaces. Further increase in c_{pol} to 7.0×10^{-4} g/mL did not change the onset of repulsion of ca. 550 Å, although the polymer layers were somewhat less compliant and hysteresis measured on approach and separation of the surfaces was weaker than that observed in the 0.5×10^{-4} g/mL polymer solutions.

Shear Forces. The shear properties of the PHLG multilayers were studied in two series of experiments. In the first series, oscillatory shear with a constant velocity (OSCV) was applied to the polymer layer confined between the mica surfaces. In the second series, a finite lateral displacement was applied to the polymer layer, and stress relaxation was monitored in time.

The typical shear traces obtained in OSCV studies are shown in Figure 4a−c. In these experiments, the lateral displacement of the top mica surface periodically changed in a triangular mode (bottom traces), reflecting its uniform back and forth motion. The top traces in Figure 4a−c display the shear response of the compressed PHLG layer. In Figure 4a, the shear force after its initial fast increase reached a plateau value, F_s. In this stage of shear, the deflection of the vertical spring remained constant due to equilibrium with viscous dissipation force and shear in the layer was dominated

by sliding. The magnitude of the critical shear force was proportional to the shear velocity, v_s. Figure 4b shows a "solid" response of the layer when the top and the bottom surfaces were coupled through a strongly compressed polymer layer: no sliding in the layer occurred, and the bottom and the top surface moved together.

For the strongly compressed polymer layers significant time was required to reach the plateau value of the shear force, and the reversal in the direction of motion of the top surface could occur before F_s was reached. Under these conditions, the plateau regime was not developed, and the shear traces showed the features resembling both the "plateau" and the "solid" response. To extract any useful information in such experiments, either the shear velocity was reduced or the value of F_s was obtained by extrapolation of the shear force to the plateau value.

Figure 4c shows a stick−slip shear response, characteristic for strongly confined PHLG layers. The stick−slip response appeared when the shear stress exerted onto the layer exceeded a critical yield stress. While the solidlike response shown in Figure 4b did not provide useful information for polymer characterization, the measurements conducted in the stick−slip regime gave the critical shear stress corresponding to shear-induced liquification of the confined polymer multilayer.

Generally, for strong polymer−surface interactions the shape of the shear traces correlated with extent of compression of adsorbed PHLG multilayers. Upon progressive confinement, the shear response measured for a particular shear velocity changed along the following path: no detectable response above the noise level → "plateau" response → underdeveloped "plateau" response → solidlike response. The stick−slip response was generally observed when a large lateral displacement was applied to the layer in the solidlike regime.

While the study of stick−slip shear properties of the confined PHLG layers is a subject of a different publication,[20] the results obtained in the "plateau" regime were analyzed by extracting F_s as the difference between the shear force at $t = t_0$ and $t = t_{plateau}$. Then, the effective viscosity of the confined polymer layer, η_{eff}, was calculated as[9c]

$$\eta_{eff} \approx \frac{16\pi}{5} R v_s F_s \ln\left(\frac{R}{D}\right) \qquad (1)$$

The sensitivity in measuring η_{eff} in these experiments was ca. 0.2 Pa·s.

Figure 4d shows the typical shear traces obtained in the relaxation experiments used for studies of the strongly compressed PHLG layers: a finite lateral displacement was applied to the top surface (top trace), and the relaxation of the polymer layer was monitored by measuring the decay in the shear force (bottom trace). To extract η_{eff}, the best fit of the decay in the lateral displacement vs time was found as[9c]

$$\eta_{eff} = \frac{k_{||} t}{\frac{16\pi}{5} R \ln\left(\frac{R}{D}\right) \ln\left(\frac{x_0}{x(t)}\right)} \qquad (2)$$

where $x(t)$ is the time-dependent lateral displacement of the vertical springs and x_0 is the lateral displacement applied to the layer. The lower range of η_{eff} measured in the relaxation experiments was ca. 20 Pa·s due to the inertia of the capacitor detector while the upper range could be as high as 10^7 Pa·s.[9c]

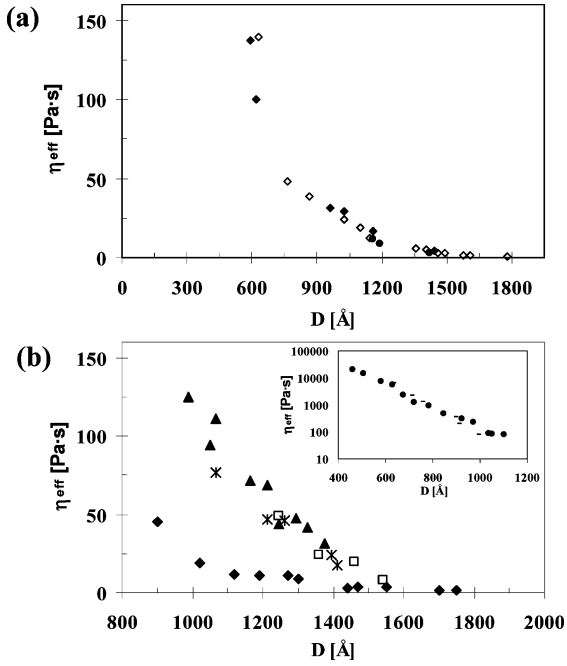

Figure 5. Variation in effective viscosity η_{eff} vs D for equilibrium PHLG layers adsorbed on the bare mica surface. (a) $c_{PHLG} = 0.5 \times 10^{-4}$ g/mL. Shear velocity, v_s, μm/s: 0.062 (●), 0.123 (◆), 0.185 (◇). (b) $c_{PHLG} = 1.0 \times 10^{-4}$ g/mL, v_s, μm/s: 0.11 (□), 0.21 (▲), 0.50 (∗), 3.50 (◆). Inset: variation in η_{eff} vs D obtained from relaxation experiments conducted for $c_{PHLG} = 1.0 \times 10^{-4}$ g/mL. Adsorption time: 4.0 h (●) and 55 ± 1 h (—).

Strong Polymer−Surface Interactions. In shear experiments conducted in 0.5×10^{-4} g/mL polymer solutions, a small negative normal force was applied to the surfaces to compensate for long-range attraction and to keep D constant. The typical shear response of the polymer layers subjected to weak and moderate compression is best represented by the shear traces in Figure 4a.

Figure 5a shows the variation in effective viscosity vs D for the equilibrium PHLG layers adsorbed from 0.5×10^{-4} g/mL polymer solutions. The shear velocity, v_s, changed from 0.062 to 0.185 μm/s by varying the shear frequency, f_s, while keeping the amplitude of shear, A_s, constant. (Increase in v_s achieved by increasing A_s resulted in a drastic decrease in η_{eff}. In addition, occasionally, large lateral displacements induced slip in the polymer layer, which did not allow for characterization of the effective viscosity of the layer.[21])

As follows from Figure 5a, a 3-fold increase in v_s did not notably change polymer viscosity. The variation in η_{eff} was more sensitive to compression of the PHLG layer. While for $D > 1500$ Å no shear force were measured above the noise level, a relatively strong increase in η_{eff} to ca. 6 Pa·s was already measured for $D \approx 1200$ Å, that is, close to the onset of attraction between the layers. Then, for 620 Å $< D <$ 1200 Å η_{eff} gradually increased, and for $D <$ 620 Å the layer became too rigid to be probed in the OSCV experiments.

For the PLHG layers adsorbed from more concentrated PHLG solutions, the shear experiments were conducted in a broader range of shear velocities by varying both f_s and A_s. Figure 5b shows a noticeable increase in η_{eff} for $D <$ 1500 Å while for $D \approx$ 1200 Å η_{eff} reached ca. 70 Pa·s. The value of η_{eff} weakly depended on shear velocity when the latter changed from 0.11 to

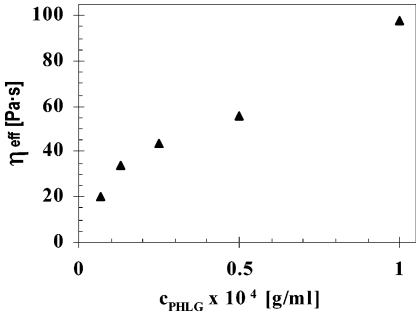

Figure 6. Variation in η_{eff} vs D measured following consecutive dilution of PHLG from $c_{PHLG} = 1.0 \times 10^{-4}$ g/mL. Shear velocity is 0.5 μm/s; $D = 1000 \pm 30$ Å.

0.5 μm/s. The reduction in η_{eff} was observed under two particular conditions. A moderate decrease in η_{eff} occurred for v_s exceeding ca. 1.0 μm/s presumably due to shear thinning in the layer (not shown): under these conditions the surfaces moved toward each other (see normal-to-shear coupling). A much stronger decrease in η_{eff} occurred for $v_s > 3.5$ μm/s, resulting from slip either in the polymer layer or at the polymer−mica interface. The slip can be distinguished from the shear thinning by their characteristic shear traces: for shear thinning F_s still showed a weak variation on shear velocity, whereas when slip occurred, F_s was almost independent of shear velocity.

Strongly compressed polymer layers were studied in relaxation experiments. The inset to Figure 5b shows the results of these experiments obtained for 350 Å < D < 1100 Å. For the PHLG layers compressed to ca. 350 Å $\eta_{eff} \approx 20\,000$ Pa·s was obtained by monitoring the decay in shear force for $t = 200$ s. A good correlation existed between the values of η_{eff} measured in OSCV and relaxation experiments: for example, for $D = 1000$ Å the difference between the values of η_{eff} was less than 10%.

The variation in η_{eff} of the PHLG layers following consecutive dilution of the polymer solution is shown in Figure 6, where η_{eff} is plotted as a function of c_{PHLG} for $D = 1000$ Å. The dilution gradually changed the value of η_{eff} from ca. 98 to 19 Pa·s. Weak attraction between the surfaces appearing in 0.7×10^{-4} g/mL PHLG solution did not result in any strong viscosity change. Again, for moderately compressed layers good agreement was obtained between the values of η_{eff} measured in the OSCV and relaxation experiments: for $D \approx 1130$ Å and 1:4 dilution η_{eff} was ca. 17 and 21 Pa·s, respectively. However, for $D = 971$ Å the value of η_{eff} obtained in relaxation experiments was notably higher than that measured in OSCV experiments, possibly due to a substantial error acquired by extrapolation of F_s to its plateau value.

Weak Polymer−Surface Interactions. Shear properties of the PHLG layers confined between the OTS-modified mica surfaces were characterized by the variation of the critical shear force.[22] When the applied shear force exceeded a critical value, the magnitude of F_s was almost insensitive to the variation in v_s, as shown in Figure 7a−c. The magnitude of the critical shear force remained at 16 ± 1.3 μN following a 20-fold increase in v_s. This effect was observed when v_s was controlled by changing either frequency, or amplitude, or both shear parameters.

However, when the applied shear displacement (and the applied force) were below the critical value, a

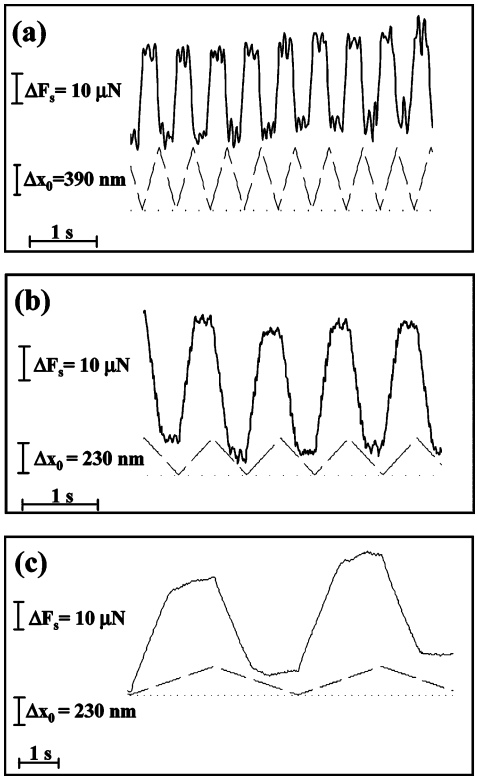

Figure 7. Typical shear traces obtained for the equilibrium PHLG layers confined between the OTS-modified mica surfaces (for description, see figure caption to Figure 4): (a) $v_s = 1.56$ μm/s; (b) $v_s = 0.23$ μm/s; (c) $v_s = 0.091$ μm/s. $D = 51 \pm 3$ Å, $c_{PHLG} = 0.5 \times 10^{-4}$ g/mL.

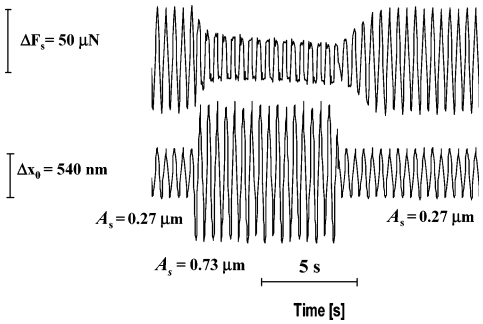

Figure 8. Characteristic shear traces measured for PHLG layer adsorbed to OTS-modified mica surfaces from 7.0×10^{-4} g/mL PHLG solution. Bottom trace: time dependence of lateral displacement applied to the top surface. Top trace: time-dependent variation in shear force. $D = 52 \pm 3$ Å. The shear response of the layer reduces when shear velocity increases.

pronounced difference in shear response was observed for different shear velocities. Figure 8 illustrates this effect for the PHLG layer adsorbed to OTS-modified mica. For $0 < t < 2.8$ s, $v_s = 0.54$ μm/s, and $A_s = 0.27$ μm the shear response of the layer was substantially stronger than for $v_s = 1.46$ μm/s and $A_s = 0.73$ μm (2.8 s < t < 11.0 s). This feature was reversible: when the shear velocity was reduced to 0.54 μm/s, the shear response of the layer was fully recovered. The decrease in shear force occurred very fast; a somewhat longer time period, however, on the order of 1 s was needed to recover the original shear response of the polymer.

The variation in F_s vs D for the PHLG layers formed from 0.5×10^{-4} and 7.5×10^{-4} g/mL polymer solutions is shown in Figure 9. The onset of shear forces at 550 $\pm$ 20 Å was very close to the onset of osmotic repulsion between the layers. The critical shear force was slowly

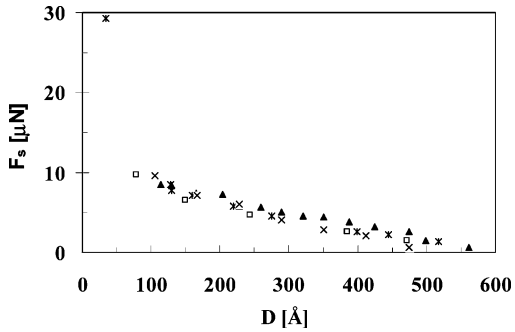

Figure 9. Variation in critical shear force, F_s, vs D in equilibrium PHLG layers adsorbed to the hydrophobized mica surface. $c_{PHLG} = 0.5 \times 10^{-4}$ g/mL (∗), $v_s = 0.46$ μm/s; $c_{PHLG} = 7.0 \times 10^{-4}$ g/mL, $v_s = 1.56$ μm/s (▲); $v_s = 0.91$ μm/s (×); $v_s = 0.46$ μm/s (□).

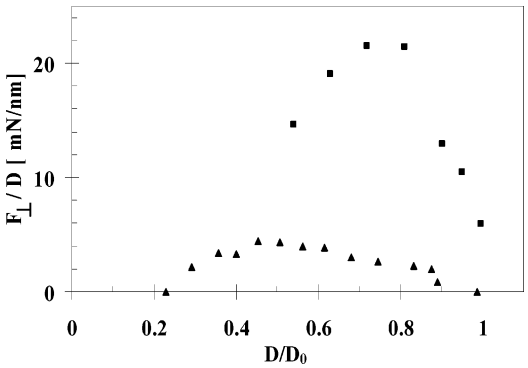

Figure 10. Coupling of normal and shear forces plotted as $F_\perp/D = k_\perp \Delta D/D$ vs compression of the layer, D/D_0, where D_0 is the onset of shear force, for equilibrium PHLG layers adsorbed to bare mica at $c_{PHLG} = 1.0 \times 10^{-4}$ g/mL, $v_s = 0.61$ μ/s (■) and to hydrophobized mica at $c_{PHLG} = 7.0 \times 10^{-4}$ g/mL, $v_s = 1.6$ μm/s (▲).

increasing up to ca. 10 μN for 550 Å ≤ D ≤ 100 Å, and it rapidly reached ca. 20 μN for stronger compression. However, even for the strongly compressed layers, the shear response of the layer was substantially weaker than for PHLG adhering to bare mica. For example, for $D = 28 \pm 3$ Å, F_s was ca. 30 μN as compared to $F_s =$ 100 μN measured for the PHLG adsorbed to bare mica and compressed to the same thickness.

Normal-to-Shear Coupling. This effect was observed for both weak and strong polymer−surface interactions. When the equilibrium PHLG layers were sheared for a relatively long time or with a relatively high shear velocity, the confining surfaces instantaneously moved inward. After shear stopped or when v_s decreased, the surfaces partly or completely returned to their original position. For the same shear velocity, the reversibility of normal-to-shear coupling depended on extent of compression. Thick PHLG layers did not easily recover after cessation of shear. Strongly compressed polymer-covered surfaces sometimes adhered when they moved inward, and they also did not easily separate when shear stopped. Quantitatively, normal-to-shear coupling was characterized by the normal force, $F_\perp$, associated with the surface motion "in" as $F_\perp = k_\perp \Delta D$, where ΔD is the normal displacement of the surfaces and $k_\perp$ is the horizontal spring constant. The variation in the normalized force, $F_\perp/D$, was plotted as a function of compression of the layer calculated as D/D_0, where D is the thickness of the layer prior to surface motion inward and D_0 is the distance between the surfaces corresponding to onset of shear forces. In Figure 10, the normalized

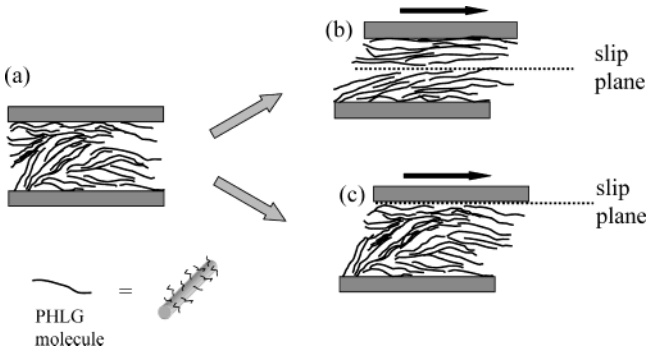

Figure 11. (a) Schematics of adsorbed PHLG multilayers confined between mica surfaces. (b) Shear of surface gel confined between bare mica (strong polymer−surface interactions). Viscous dissipation occurs in the PHLG layer. (c) Shear of surface gel confined between hydrophobically modified mica (weak polymer−surface interactions). The shear plane is at the polymer−substrate.

normal-to-shear coupling forces obtained for strong and weak polymer surface interactions showed the maxima for a particular extent of polymer compression. Second, the magnitude of $F_\perp/D$ was significantly larger for the polymer adsorbed to bare mica. Finally, for the PHLG layer strongly and weakly adhering to the substrate the maxima in $F_\perp/D$ were obtained for extent of compression 0.8 and 0.45, respectively.

Discussion

The length and diameter of the individual rigid-rod molecules of polypeptides with $M_W = 60\,500$ are on the order of 40 nm and 15−20 Å,[3,4,7a] respectively. Thus, it can be concluded that PHLG formed multilayers following its adsorption on bare and hydrophobized mica. In the multilayers the individual PHLG molecules associated side-to-side through dipole−dipole interactions;[4,7a] as a result, a physical surface network typical for polymers with inherent rigidity was formed,[1,3c] as shown in Figure 11a.

The effect of polymer−surface interactions on the normal and shear properties of the surface network is the main finding of the present work. While partial PHLG aggregation in solution cannot be ruled out, by comparing the force profiles in Figures 1 and 3, we conclude that polymer supramolecular assembly on the substrate was dominated by polymer−surface rather than polymer−polymer interactions. Indeed, the thickness of the polymer multilayer on bare mica (strong polymer−surface interactions) was 3 times as large as the thickness of the polymer multilayer adhering to the OTS-modified surface (weak polymer−surface interactions). Since polypeptide adsorption on mica is driven by electrostatic interactions between the polymer dipoles and the charged substrate,[7] screening of the surface charge with OTS strongly diminished the driving force for adsorption. Under these conditions, limited polymer adsorption on hydrophobized mica could occur via weak interactions between the PHLG side chains and octadecyl chains of OTS,[7b] and the equilibrium layer thickness was achieved for lower c_{PHLG} and after shorter adsorption time.

Although PHLG is an associative polymer,[1,3,4] no attraction was measured between the surfaces densely covered with PHLG multilayers. Attraction between the polymer-covered surfaces was observed only in 0.5×10^{-4} g/mL PHLG solutions confined between the bare

mica surfaces. The energy of attraction estimated from Derjaguin's approximation $E \approx 2\pi F/R$ was about 3600 μN/m, which compared well with the energy of attraction measured for the two bare mica surfaces in toluene.[23b] However, attraction commenced at 1300 Å, which was significantly farther than the onset of attraction of mica in toluene. The long-range attraction force measured between the surfaces following their 24 h exposure to 0.5×10^{-4} g/mL PHLG solution could result from the electrostatically driven bridging between the clusters of PHLG molecules on one surface[7a] and the islands of bare mica on the opposite surface. Additional support for the bridging origin of attraction followed from Figure 1: the onset of repulsion of 425 ± 25 Å measured in 0.5×10^{-4} g/mL PHLG solution roughly corresponded to half of the distance 800 ± 50 Å, the onset of strong repulsion for 7.5×10^{-4} g/mL solution. Furthermore, for the polymer adsorbed to the OTS-modified substrate no attraction was observed in the entire range of polymer concentrations in the bulk.

The formation of the polymer surface network was further supported by the results of "dilution" experiments. The association of macromolecules in the multilayers led to the detachment of *assemblies* of macrochains from the surface rather than desorption of individual molecules. Therefore, the process of desorption was significantly slower than the corresponding adsorption process. Attraction between the surfaces reappearing upon significant dilution indicated that islands of the bare mica surface appeared in the polymer-covered substrate. In this case, a low magnitude of attraction force and a large value of D corresponding to steep repulsion indicated that desorption was not complete and that only a limited fraction of the mica surface contributed to bridging.

Shear Properties. Since PHLG macromolecules formed a surface network, their shear properties can be best described as those of a weak physical gel whose structure is shown in Figure 11a. For strong and weak polymer−surface interactions some similarity in the shear properties of the surface gel was observed. By contrast with polymer brushes[23] and polymers adsorbed from a good solvent,[24] for adsorbed PHLG layers the onsets of the normal and shear forces were relatively close.[25] This feature originated from the associative nature of PHLG and from the "open" structure of the polymer network whose extent of interpenetration in the gap strongly increased with compression (Figure 11b). Furthermore, under particular conditions, such as increase in shear velocity or long-time shear, PHLG layers adsorbed to both bare and hydrophobized mica could feature slip or shear thinning. Nevertheless, polymer−surface interactions had the biggest impact on the shear properties of the adsorbed PHLG network. Therefore, shear of strongly and weakly adsorbing PHLG gels will be discussed separately.

For strong polymer−surface interaction, forces of a hydrodynamic origin dominated the shear response of the layer, and its rheological properties could be characterized by effective viscosity. Good correlation was obtained in measurements of normal and shear forces. For $c_{PHLG} = 0.5 \times 10^{-4}$ g/mL, a notable increase in η_{eff} occurred relatively close to the onset of attraction between the surfaces. The second steep increase in η_{eff} measured for $D = 600 \pm 25$ Å was close to the onset of repulsion in the normal force profile. This increase in effective viscosity resulted from the growth of polymer concentration in the gap and strong energy dissipation in the interpenetrating surface networks.

For the surface gel formed at $c_{PHLG} \geq 1.0 \times 10^{-4}$ g/mL, a denser structure of the polymer surface network formed from the more concentrated PHLG solution, resulting in a higher effective viscosity and stronger viscous dissipation in the layer in comparison with the surface gel adsorbed from 0.5×10^{-4} g/mL PHLG solution. For example, for $D = 600$ Å η_{eff} was ca. 150 and 8000 Pa·s for PHLG adsorbed from 0.5×10^{-4} and 1.0×10^{-4} g/mL, respectively.

The variation of effective viscosity of the polymer with increase of v_s could be used for further characterization of the surface gel; however, η_{eff} showed a rather weak change, perhaps due to the insufficient range of v_s needed to probe viscoelasticity of the layer.[26] On the other hand, significant increase in v_s dramatically reduced η_{eff} by inducing shear thinning (see below) and slip in the layer.

For the polymer layer adsorbed to hydrophobized mica, a complex variation in F_s with v_s below and above the critical applied shear force (Figures 7 and 8, respectively) indicated that slip at the polymer−substrate interface dominated shear of the gel (Figure 11c). Recently, surface slip studied in the configuration of the SFB was reported by several groups.[27] In contrast to the present work, most of these studies focused on the measurements of a hydrodynamic force appearing in response to the variation in surface separation. This approach is quite different than the experiments described in the current paper.

Despite the fact that slip complicated the study of the intrinsic properties of PBLG surface gel, some conclusions can still be made on the basis of shear experiments. The onset of distinguishable shear forces was similar for the layers formed from 0.5×10^{-4} and 7.0×10^{-4} g/mL PHLG solutions, giving another indication that the equilibrium polymer layer was adsorbed to the hydrophobized surface exposed to dilute solutions. For 200 Å $< D <$ 500 Å a rather weak variation in F_s with D was observed, dominated by polymer slip on the surface. A notable increase in F_s occurred for $D \approx 100$ Å, corresponding to the strong increase in normal forces; this effect was caused by forced polymer adsorption to the surface, which suppressed surface slip and increased the shear force in the layer.

The existence of slip at the polymer−surface boundary explained the dependence of shear response on shear velocity in Figures 7 and 8. For small shear amplitudes (Figure 8) the surfaces were coupled through a strongly compressed rigid polymer layer. However, increase in shear amplitude generated partial slip at the polymer-hydrophobized mica interface, and the shear response of the layer decreased. When A_s decreased to its initial value, ca. 1 s was required to recover polymer−surface bonding.

Normal-to-Shear Coupling. While partial removal of the polymer from the gap between the surfaces could occur for the weakly compressed PHLG layers, the reversibility of the surface motion "in" and "out" for the moderately compressed polymer indicated that a different effect was responsible for normal-to-shear coupling. Normal-to-shear coupling for strongly adsorbing gellike layers originated from their shear thinning: long-time shear or high-velocity shear destroyed noncovalent cross-links between the PHLG fibrils or individual polymer molecules, which strongly decreased

polymer effective viscosity. As a result, the layer could not sustain the applied normal load and the surfaces moved inward. It should be noted that, in principle, a similar effect could be observed for the surface gel weakly adsorbing to the hydrophobized surface; however, increase in shear velocity promoted surface slip, and the weak motion of the surfaces toward each other was rather caused by the rearrangement of PHLG molecules at the polymer−surface interface.

The existence of maxima in the force profiles in Figure 10 can be explained as follows. For $D/D_0 > 1$, no normal or shear interactions could be detected; thus, the normal-to-shear coupling was zero. On the other hand, in strongly compressed rigid polymer layers shear thinning and surface sliding were suppressed. For moderate compression of PHLG adsorbed to bare mica, the variation in $F_\perp/D$ originated mostly from the nonuniform structure of the surface gels: a more compact inner layer strongly adhering to the surface and the outer layer with a weaker structure. Shear thinning occurred mostly in the outer layer which led to a pronounced maximum in $F_\perp/D$ vs D/D_0. A more uniform structure of the polymer gel weakly adsorbing to the OTS-modified mica could, in principle, explain a more gradual variation in $F_\perp/D$. However, since slip dominated shear in such layers, the existence of a weak maximum presumably reflected the extent of molecular rearrangement at the polymer−substrate interface as a function of layer compression.

Conclusions

This work shows that rigid-rod associative polymer poly(*n*-hexyl-L-glutamate) forms weak surface gels on hydrophilic and hydrophobic surfaces (providing strong and weak polymer−surface interactions, respectively). The nature of the surface plays a major role in the properties of adsorbed multilayers. The equilibrium PHLG layers adsorbed to the bare mica substrate are significantly thicker than those on the OTS-modified surface. For strong polymer−surface interaction, the structure of the surface network is more compact, and upon shearing strong viscous dissipation occurs in the layer. In contrast, shear of the surface gel formed on the hydrophobic substrate is dominated by surface slip; therefore, the shear properties of this surface gel cannot be described by effective viscosity. Under particular conditions, such as long-time shear or high shear velocity, the adsorbed polymer strongly interacting with the substrate undergoes shear thinning, consistent with the nature of a weak physical gel.

The attraction force between the polymer-covered surfaces is measured only for unsaturated polymer layers. This fact is explained by bridging between the polymer adsorbed to one surface and the islands of bare mica on the other surface. For the layers adsorbed from more concentrated solutions, osmotic repulsion governs interactions between the surfaces.

References and Notes

(1) Hvidt, S.; Heller, K. In *Physical Networks. Polymers and Gels*; Burchard, W., Ross-Murphy, S. B., Eds.; Elsevier Applied Science: London, 1988; pp 195−208.
(2) Seo, M.; Kumacheva, E. *Colloid Polym. Sci.* **2002**, *280*, 607−615. Revol, J.-F.; Bradford, H.; Giasson, J.; Marchessault, R. H.; Gray, D. G. *Int. J. Biol. Macromol.* **1992**, *14*, 170−172.
(3) Russo, P. S.; Miller, W. G. *Macromolecules* **1984**, *17*, 1324−1331. (b) Murthy, A. K.; Muthukumar, M. *Macromolecules* **1987**, *20*, 564−569. (c) Cohen, Y. *J. Polym. Sci., Part B: Polym. Phys.* **1996**, *34*, 57−64.
(4) Block, H. *Poly (γ-benzyl-L-glutamate) and Other Glutamic Acid Containing Polymers*; Gordon and Breach: New York, 1983; p 64.
(5) Hartmann, L.; Kratzmuller, T.; Braun, H.-G.; Kremer, F. *Macromol. Rapid Commun.* **2000**, *21*, 814−819.
(6) Wolff, O.; Seydel, E.; Johannsmann, D. *Faraday Discuss.* **1997**, *107*, 91−104.
(7) Kitaev, V.; Schillen, K.; Kumacheva, E. *J. Polym. Sci., Part B: Polym. Phys.* **1998**, *36*, 1567−1577. (b) Kitaev, V.; Kumacheva, E. *Langmuir* **1998**, *14*, 5568−5572. (c) Sohn, D.; Kitaev, V.; Kumacheva, E. *Langmuir* **1999**, *15*, 1698−1702.
(8) Fukuto, M.; Heilmann, R. K.; Pershan, P. S.; Yu, S. M.; Griffiths, J. A.; Tirrell, D. A. *J. Chem. Phys.* **1999**, *111*, 9761−9777.
(9) Israelachvili, J. *J. Colloid Interface Sci.* **1973**, *44*, 259−272. (b) Kumacheva, E. *Prog. Surf. Sci.* **1998**, *58*, 75−120. (c) Klein, J. Kumacheva, E. *J. Chem. Phys.* **1998**, *108*, 6996−7009.
(10) Leckband, D. *Nature (London)* **1995**, *376*, 617−618.
(11) Luckham, P. F.; Klein, J. *J. Chem. Soc., Faraday Trans. 1* **1984**, *80*, 865−878.
(12) Gauthier-Manuel, B.; Gallinet, J.-P. *Phys. Chem.* **2001**, *3*, 1089−1092. (b) Gauthier-Manuel, B.; Gallinet, J.-P. *J. Colloid Interface Sci.* **1995**, *175*, 476−483.
(13) Nylander, T.; Wahlgren, N. M. *Langmuir* **1997**, *13*, 6219−6225.
(14) Blomberg, E.; Claesson, P. M.; Froberg, J. C. *Biomaterials* **1998**, *19*, 371−386.
(15) Abe, T.; Kurihara, K.; Higashi, N.; Niwa, M. *J. Phys. Chem.* **1995**, *99*, 1820−1823. (b) Abe, T.; Higashi, N.; Niwa, M.; Kurihara, K. *Langmuir* **1999**, *15*, 7725−7731.
(16) Schmitt, F. J.; Yoshizawa, H.; Schmidt, A.; Duda, G.; Knoll, W.; Wegner, G.; Israelachvili, J. N. *Macromolecules* **1995**, *28*, 3401−3410.
(17) Kessel, C. R.; Granick, S. *Langmuir* **1991**, *7*, 532−538. (b) Ruths, M.; Granick, S. *Langmuir* **1998**, *14*, 1804−1814.
(18) Luckham, P. F.; Klein, J. *Macromolecules* **1985**, *18*, 721−728.
(19) In the SFB experiments, half of the distance corresponding to onset of repulsion generally gives the thickness of adsorbed layer.
(20) Kitaev, V.; Kumacheva, E. Manuscript in preparation.
(21) Macosko, C. W. *Rheology: Principles, Measurements and Applications*; VCH: New York, 1994; p 194.
(22) The rate of increase in the shear force differed by less than 5% from the rate of increase of the applied shear force, thus precluding the estimation of effective viscosity of the layer.[20] However, when the magnitude of the critical shear force was reached, the initial sharp increase of the shear force was either leveled or oscillated, revealing stick−slip motion.
(23) Klein, J.; Kumacheva, E.; Mahalu, D.; Perahia, D.; Fetters, L. J. *Nature (London)* **1994**, *370*, 634−636. (b) Klein, J.; Kumacheva, E.; Mahalu, D.; Perahia, D.; Fetters, L. J. *Faraday Discuss.* **1994**, *98*, 173−188.
(24) Raviv, U.; Tadmor, R.; Klein, J. *J. Phys. Chem. B* **2001**, *105*, 8125−8134.
(25) In experiments with higher PHLG concentrations, shear response could be detected at surface separations larger than the onset of normal repulsion due to hydrodynamic friction of viscous polymer solutions confined to less than a micron.
(26) When *sinusoidal* oscillatory shear was applied to the adsorbed PHLG layer, a clear phase shift was observed between applied and resulting lateral displacements, which was strongly dependent on extent of the layer compression (manuscript in preparation).
(27) Zhu, Y.; Granick, S. *Macromolecules* **2002**, *35*, 4658−4663. (b) Vinogradova, O. I.; Horn, R. G. *Langmuir* **2001**, *17*, 1604−1607. (c) Vinogradova, O. I. *Langmuir* **1998**, *14*, 2827−2837.

MA025675W